Physics Letters A 383 (2019) 1879–1887

Contents lists available at ScienceDirect

Physics Letters A

www.elsevier.com/locate/pla

A new lattice hydrodynamic model accounting for the traffic interruption probability on a gradient highway

Qingying Wang [a,b,c], Rongjun Cheng [a,b,c,*], Hongxia Ge [a,b,c]

[a] Faculty of Maritime and Transportation, Ningbo University, Ningbo 315211, China
[b] Jiangsu Province Collaborative Innovation Center for Modern Urban Traffic Technologies, Nanjing 210096, China
[c] National Traffic Management Engineering and Technology Research Centre, Ningbo University Sub-centre, Ningbo 315211, China

ARTICLE INFO

Article history:
Received 25 February 2019
Received in revised form 15 March 2019
Accepted 15 March 2019
Available online 20 March 2019
Communicated by C.R. Doering

Keywords:
Traffic flow
Lattice hydrodynamic
The traffic interruption probability
Gradient highway

ABSTRACT

In this paper, a novel lattice hydrodynamic model is presented by accounting for the traffic interruption probability on a gradient highway. The stability condition can be obtained by the use of linear analysis. Linear analysis demonstrates that the traffic interruption probability and the slope will affect the stability region. Through nonlinear analysis, the mKdV equation is derived to describe the phase transition of traffic flow. Furthermore, the numerical simulation is carried out, and the results are consistent with the analytical results. Numerical results demonstrate that the traffic flow can be efficiently improved by accounting for the traffic interruption probability on a gradient highway.

1. Introduction

On urban residents' daily lives, traffic jams have attached wide attention amongst scientists and researchers. In order to investigate the properties of traffic jams and alleviate it, various traffic models have been put forward, which include car-following models [1–12], cellular automation models [13,14], macro traffic models [15–23], lattice hydrodynamic models [24–30] and so on.

According to the observed headway, drivers adjust their velocity. With the consideration of it, Nagatani [31] firstly put forward a lattice hydrodynamic model in 1998. As the traffic environment changes and time goes by, the traffic flow becomes more complex. On the basis of it, many extended lattice hydrodynamic models have been proposed. These novel models consider different factors like backward looking effect [32–35], the optimal velocity difference effect [36–40], the traffic flow difference effect [41,42], the self-anticipative density effect [43,44] etc. However, it is not difficult to find that many models consider the situation of vehicles on a single lane. While in actual traffic system, driving environments also have a certain impact on traffic congestions, such as two-dimensional lattice models [45–49], curved roads [50–52], triangular lattice models [53,54].

What's more, the traffic models on a gradient highway are also worth studying. In 2014, Gupta et al. [55] put forward a new lattice model on a gradient highway, which considered the effect of optimal velocity difference. Komada [56] proposed a car-following model accounting for the effect of gravitational force upon traffic flow with gradients in 2009. Also, Sun et al. [57] presented an extended car-following model with considering drivers' characteristics on a gradient highway. Zhu [58] proposed a car-following model on a gradient highway, it showed that the slope plays an important role in influencing the tendency of density waves in different traffic flow regions. Actually, it is rare to study the influence of the traffic interruption probability on a gradient highway. Based on it, an extended lattice hydrodynamic model will be proposed to investigate its impact on traffic flow.

The paper is organized as follows: in the following section, the improved lattice hydrodynamic model is proposed, which considers the effect of the traffic interruption probability on a gradient highway. In section 3, the linear stability analysis is performed, and the stability condition can be obtained. The nonlinear analysis and the solution of the mKdV equation are derived in section 4. In section 5, the numerical simulation is carried out to verify the analysis results and conclusions are given in section 6.

* Corresponding author at: Faculty of Maritime and Transportation, Ningbo University, Ningbo 315211, China.
E-mail address: chengrongjun@nbu.edu.cn (R. Cheng).

https://doi.org/10.1016/j.physleta.2019.03.019
0375-9601/

2. The extended lattice hydrodynamic model

To analyze the density of traffic flow on a single lane, Nagatani [31] proposed a lattice hydrodynamic model firstly with the considerations of car-following models and macroscopic models in 1998, which is described by the following equations:

$$\partial_t \rho + \rho_0 \partial_x \rho v = 0 \tag{1}$$

$$\partial_t \rho v = a\rho_0 V\left(\rho\left(x+\delta\right)\right) - a\rho v \tag{2}$$

where ρ_0 indicates the average density, a represents driver's sensitivity, ρ and v respectively denote the traffic density and velocity, δ is the average headway, and it is the inverse of ρ_0, $\rho(x+\delta)$ is the local density at position $x+\delta$.

Then, with dimensionless space x (let $x^* = x/\delta$, and x^* is indicated as x hereafter), the above model is modified and rewritten with its lattice version as follows:

$$\partial_t \rho_j + \rho_0\left(\rho_j v_j - \rho_{j-1} v_{j-1}\right) = 0 \tag{3}$$

$$\partial_t \rho_j v_j = a\rho_0 V\left(\rho_{j+1}\right) - a\rho_j v_j \tag{4}$$

where j denotes the lattice number, v_j is the local velocity and ρ_j represents the local density of lattice j at time t, respectively. $V(\cdot)$ is called the optimal velocity function, it is a function of local density. With an inflection point at critical density, $V(\cdot)$ is showed by a monotonically decreasing function. The optimal velocity function [52] can be adopted as follows:

$$V\left(\rho_j(t)\right) = \frac{v_{\max}}{2} \times\left[\tanh\left(\frac{2}{\rho_0} - \frac{\rho_j(t)}{\rho_0^2} - \frac{1}{\rho_c}\right) + \tanh\left(\frac{1}{\rho_c}\right)\right] \tag{5}$$

where ρ_c indicates the critical density, $v_{\max}$ means the maximum velocity.

The above model is further improved to account for the effect of traffic interruption probability by Peng et al. [59]. By considering the difference of optimal traffic flow on site of j and $j+1$, the continuity equation remains preserved while the evolution equation is modified. However, the change of traffic flow is continuous in real traffic, and it plays an important role in stabilizing the traffic flow. On the basis of it, a new lattice hydrodynamic model can be proposed as follows:

$$\begin{aligned}\partial_t \rho_j v_j &= a\rho_0 V\left(\rho_{j+1}\right) - a\rho_j v_j \\ &+ a\int_{t-\tau_0}^{t}\left[-\alpha_1 p \rho_j(s) v_j(s)\right. \\ &\left.+\alpha_2(1-p)\left(\rho_{j-1}(s) v_{j-1}(s) - \rho_j(s) v_j(s)\right)\right] ds\end{aligned} \tag{6}$$

where τ_0 is the time step, p is the interrupted probability that the traffic flow of lattice on site $j+1$, α_1 and α_2 are the reactive coefficients.

There is no doubt that more and more factors affecting traffic congestion are taken into consideration and comprehensive in the study of continuous improvement of traffic model. However, it is worth noting that in the study of traffic flow, we need to consider not only drivers' factors, but also the impact of geographical environment on the stability of traffic flow, such as the effect of slope. Fig. 1 shows the illustration of gravitational force acting upon a vehicle on an uphill and downhill highway. θ is the slope of a gradient road, g denotes the gravitational acceleration and m is the total mass of the vehicle on the lattice. And the gravitational force generates a force $mg\sin\theta$ paralleling to the road on gradient roads,

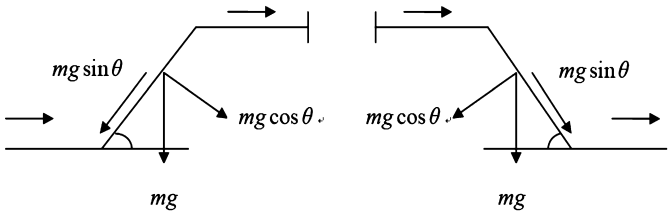

Fig. 1. An illustration of gravitational force upon a vehicle on a gradient highway: uphill and downhill.

which can reduce or enhance the maximal speed of the vehicle. On the basis of the effect of traffic interruption probability, a new evolution equation for an extended lattice hydrodynamic model can be proposed, which is to describe the movement of vehicles on a single lane gradient highway can be obtained:

$$\begin{aligned}\partial_t \rho_j v_j &= a\rho_0 V\left(\rho_{j+1}, \theta\right) - a\rho_j v_j \\ &+ a\int_{t-\tau_0}^{t}\left[-\alpha_1 p \rho_j(s) v_j(s)\right. \\ &\left.+\alpha_2(1-p)\left(\rho_{j-1}(s) v_{j-1}(s) - \rho_j(s) v_j(s)\right)\right] ds\end{aligned} \tag{7}$$

$$\partial_t \rho_j + \rho_0\left(\rho_j v_j - \rho_{j-1} v_{j-1}\right) = 0 \tag{8}$$

The optimal velocity function can be got as follows:

$$V(\rho,\theta) = \frac{V_{f,\max} - V_{g,u,\max}}{2} \times\left[\tanh\left(\frac{1}{\rho} - \frac{1}{\rho_{c,u,\theta}}\right) + \tanh\left(\frac{1}{\rho_{c,u,\theta}}\right)\right] \tag{9}$$

for an uphill gradient road, and

$$V(\rho,\theta) = \frac{V_{f,\max} + V_{g,d,\max}}{2} \times\left[\tanh\left(\frac{1}{\rho} - \frac{1}{\rho_{c,d,\theta}}\right) + \tanh\left(\frac{1}{\rho_{c,d,\theta}}\right)\right] \tag{10}$$

for a downhill gradient road, where $V_{f,\max}$ means the maximal velocity on the road without any slope, $V_{g,u,\max}$ is the maximal reduced velocity on uphill, and $V_{g,d,\max}$ is the maximal enhanced velocity on downhill gradient roads, which can be formulated as follows:

$$V_{g,u,\max} = V_{g,d,\max} = \frac{mg}{\mu}\sin\theta \tag{11}$$

where μ is a longitudinal friction coefficient, and we choose $\mu = mg$. $\rho_{c,u,\theta} = 1/h_{c,u,\theta}$ and $\rho_{c,d,\theta} = 1/h_{c,d,\theta}$, they are the inverse of the safety distance for the vehicle on the uphill and downhill. Also, in the process of vehicle operation, the speed will change in an uphill (downhill) situation. And we can get the equations as follows:

$$h_{c,u,\theta} = h_c\left(1 - \xi\sin\theta\right) \quad \text{and} \quad h_{c,d,\theta} = h_c\left(1 + \eta\sin\theta\right) \tag{12}$$

where ξ and η are constant and we take $\xi = \eta = 1$. Then the optimal velocity can be integrated as follows:

$$V(\rho,\theta) = \frac{V_{f,\max} - V_{g,\max}}{2} \times\left[\tanh\left(\frac{1}{\rho} - \frac{1}{\rho_{c,u}}\right) + \tanh\left(\frac{1}{\rho_{c,u}}\right)\right] \tag{13}$$

where $V_{g,\max} = V_{g,u,\max}$, $\rho_{c,u} = 1/h_{c,u}$, $h_{c,u} = h_c\left(1 - \sin\theta\right)$, the uphill and downhill can be presented the positive and negative θ. We take $-6^\circ \le \theta \le 6^\circ$. The optimal velocity function can be obtained:

$$V(\rho,\theta)=\frac{V_{f,\max}-\sin\theta}{2}V_0(\rho,\theta) \tag{14}$$

where $V_0(\rho,\theta)$ is adopted by the symmetry of density as follows:

$$V_0(\rho,\theta)=\tanh\left(\frac{2}{\rho_0}-\frac{\rho}{\rho_0^2}-\frac{1-\sin\theta}{\rho_c}\right)+\tanh\left(\frac{1-\sin\theta}{\rho_c}\right) \tag{15}$$

By taking the difference form of (7) and (8) and eliminating speed v_j, the density equation is obtained:

$$\begin{aligned}&\partial_t^2\rho_j(t)+a\partial_t\rho_j(t)+a\rho_0^2A(\theta)\left[V_0\left(\rho_{j+1},\theta\right)-V_0\left(\rho_j,\theta\right)\right]\\&+a\alpha_1p\left[\rho_j(t)-\rho_j(t-\tau_0)\right]\\&-a\alpha_2(1-p)\left[\rho_{j+1}(t)-\rho_{j+1}(t-\tau_0)-\rho_j(t)+\rho_j(t-\tau_0)\right]\\&=0\end{aligned} \tag{16}$$

where $A(\theta)=\dfrac{V_{f,\max}-\sin\theta}{2}$.

3. Linear stability analysis

In this section, a linear stability analysis will be conducted, which is to investigate the traffic interruption probability effect on a gradient highway. It is proposed that the steady state is the uniform traffic flow with a constant density ρ_0 and optimal velocity $V(\rho_0,\theta)$. The steady-state solution of the homogeneous traffic flow can be obtained:

$$\rho_j(t)=\rho_0,\ V_0\left(\rho_j(t)\right)=V_0(\rho_0,\theta) \tag{17}$$

Let $y_j(t)$ be a small perturbation on site j. We can get:

$$\rho_j(t)=\rho_0+y_j(t) \tag{18}$$

Inserting (17) and (18) into Eq. (16), we can get the equation as follows:

$$\begin{aligned}&\partial_t^2y_j(t)+a\partial_ty_j(t)+a\rho_0^2A(\theta)V'(\rho_0,\theta)\left[y_{j+1}(t)-y_j(t)\right]\\&+a\alpha_1p\left[y_j(t)-y_j(t-\tau_0)\right]\\&-a\alpha_2(1-p)\left[y_{j+1}(t)-y_{j+1}(t-\tau_0)-y_j(t)+y_j(t-\tau_0)\right]\\&=0\end{aligned} \tag{19}$$

Expanding $y_j(t)=e^{ikj+zt}$, we can get:

$$\begin{aligned}&z^2+az+a\rho_0^2A(\theta)V'(\rho_0,\theta)\left(e^{ik}-1\right)+a\alpha_1p\left(1-e^{-z\tau_0}\right)\\&-a\alpha_2(1-p)\left(e^{ik}-e^{ik-z\tau_0}-1+e^{-z\tau_0}\right)=0\end{aligned} \tag{20}$$

Inserting $z=z_1(ik)+z_2(ik)^2+\cdots$ into (18), the first-order and second-order terms of coefficient of ik are:

$$z_1=-\frac{\rho_0^2A(\theta)V'(\rho_0,\theta)}{1+\alpha_1p\tau_0} \tag{21}$$

$$z_2=-\frac{2+a\alpha_1p\tau_0^2}{2a(1+\alpha_1p\tau_0)}z_1^2-\frac{\alpha_2(1-p)\tau_0}{1+\alpha_1p\tau_0}z_1-\frac{\rho_0^2A(\theta)V'(\rho_0,\theta)}{2(1+\alpha_1p\tau_0)} \tag{22}$$

When $z_2<0$, the uniform steady-state flow becomes unstable for the long-wavelength models. On the contrary, the uniform steady-state flow remains stable if $z_2>0$. Therefore, the stability condition for traffic flow is given by:

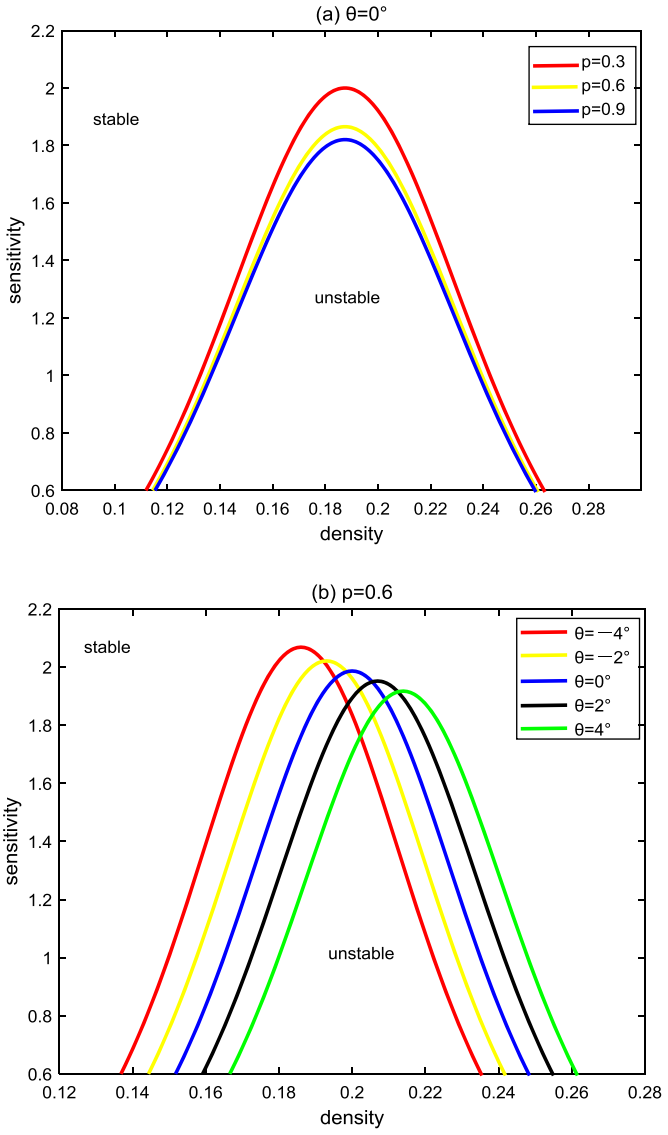

Fig. 2. The neutral stability curves for (a) $p=0.3,0.6,0.9$ with fixed $\theta=0°$. (b) $\theta=-4°,-2°,0°,2°,4°$ with fixed $p=0.6$. (For interpretation of the colors in the figure(s), the reader is referred to the web version of this article.)

$$a=-\frac{2\rho_0^2A(\theta)V'(\rho_0,\theta)}{\alpha_2\tau_0(1-p)(1+\alpha_1p\tau_0)+(1+\alpha_1p\tau_0)^2+\alpha_1p\tau_0^2\rho_0^2A(\theta)V'(\rho_0,\theta)} \tag{23}$$

The instability condition for the homogenous traffic flow is given by:

$$a>-\frac{2\rho_0^2A(\theta)V'(\rho_0,\theta)}{\alpha_2\tau_0(1-p)(1+\alpha_1p\tau_0)+(1+\alpha_1p\tau_0)^2+\alpha_1p\tau_0^2\rho_0^2A(\theta)V'(\rho_0,\theta)} \tag{24}$$

The above equation clearly shows that the traffic interruption probability and the slope θ on a gradient highway play an important role in stabilizing the traffic flow on a single lane. When $\alpha_1=\alpha_2=\theta=0$, the result of stability condition is same as the model of Nagatani [31].

For the novel lattice hydrodynamic model with the consideration of the traffic interruption probability on a gradient highway, the neutral stability lines in the parameter space (ρ,a) are shown in Fig. 2, where $\rho_0=\rho_c=0.25$, $V_{f,\max}=2$, $\alpha_1=0.5$ and $\alpha_2=0.1$. From Fig. 2 (a), it shows that the critical points will

rise with increasing value of p from 0.3 to 0.9, when $\theta = 0°$. That is to say, when the influence of slope is fixed, it is effective to stabilize the traffic flow. Fig. 2 (b) shows the situation for $\theta = -4°, -2°, 0°, 2°, 4°$, when $p = 0.3$. Positive and negative θ indicate the solution of uphill and downhill. In an uphill, the maximal flux increases when the slope increases. And with the increase of the slope, the maximal flux decreases in a downhill situation.

4. Nonlinear analysis and the mKdV equation

To describe the traffic evolution pattern of the novel model, nonlinear analysis is presented near the critical point (ρ_c, a_c) with reductive perturbation method in this section. The slow variables X and Y for $0 < \varepsilon \leq 1$ as follows:

$$X = \varepsilon(j + bt), T = \varepsilon^3 t \tag{25}$$

where b is a constant. Let $\rho_j(t)$ satisfy the equation:

$$\rho_j(t) = \rho_c + \varepsilon R(X, T) \tag{26}$$

Substituting (25) and (26) into (16) and expending each team to the fifth order of ε, then we can obtain:

$$\begin{aligned}&\varepsilon^2 m_1 \partial_X R + \varepsilon^3 m_2 \partial_X^2 R + \varepsilon^4 \left(\partial_T R + m_3 \partial_X^3 R + m_4 \partial_X R^3\right) \\ &+ \varepsilon^5 \left(m_5 \partial_X \partial_T R + m_6 \partial_X^2 R^3 + m_7 \partial_X^4 R\right) = 0\end{aligned} \tag{27}$$

The coefficients $m_i\,(i = 1, 2, 3..., 7)$ are given in Table 1, where $V_0' = \dfrac{\partial V_0(\rho)}{\partial \rho} | \rho = \rho_c$ and $V_0''' = \dfrac{\partial^3 V_0(\rho)}{\partial \rho^3} | \rho = \rho_c$. Near the critical point (ρ_c, a_c), we assume the value of a_c as:

$$a_c = \left(1 + \varepsilon^2\right) a \tag{28}$$

By taking $b = -\dfrac{\rho_0^2 A(\theta) V_0'}{1 + \alpha_1 p \tau_0}$ and eliminating the second and third order terms of ε, we obtain:

Table 1
The coefficients m_i of the model.

m_1	m_2
$b + \dfrac{\rho_c^2 A(\theta) V_0'}{1 + \alpha_1 p \tau_0}$	$\dfrac{b^2 + \rho_c^2 A(\theta) V_0' - \alpha_1 p b^2 \tau_0^2 - 2a\alpha_2 (1-p) b\tau_0}{2a(1 + \alpha_1 p \tau_0)}$
m_4	m_6
$\dfrac{A(\theta) \rho_c^2 V_0'''}{6(1 + \alpha_1 p \tau_0)}$	$\dfrac{\rho_c^2 A(\theta) V_0' + \alpha_1 p b^3 \tau_0^3 - 3\alpha_2 (1-p) b\tau_0 (1 - b\tau_0)}{6(1 + \alpha_1 p \tau_0)}$
m_5	m_3
$\dfrac{2b - \alpha_2 (1-p) \tau_0}{a(1 + \alpha_1 p \tau_0)}$	$\dfrac{\rho_c^2 A(\theta) V_0' + \alpha_1 p b^3 \tau_0^3 - 3\alpha_2 (1-p) b\tau_0 (1 - b\tau_0)}{6(1 + \alpha_1 p \tau_0)}$
m_7	
$\dfrac{\rho_c^2 A(\theta) V_0'''}{12(1 + \alpha_1 p \tau_0)}$	

$$\begin{aligned}&\varepsilon^4(-g_1 \partial_X^3 R + g_2 \partial_X R^3 + \partial_T R) \\ &+ \varepsilon^5(g_4 \partial_X^4 R + g_5 \partial_X^2 R^3 + g_3 \partial_X^2 R) = 0\end{aligned} \tag{29}$$

where the coefficients $g_i\,(1, 2, ..., 5)$ are given in Table 2.

Equation (27) can be transformed into the standard mKdV equation as follows:

$$T = \frac{1}{g_1} T', R = \sqrt{\frac{g_1}{g_2}} R' \tag{30}$$

We can obtain the modified mKdV equation with an $O(\varepsilon)$ correction term as follows:

$$\begin{aligned}\partial_{T'} R' &= \partial_X^3 R' - \partial_X R'^3 \\ &+ \varepsilon \left[\frac{g_3}{g_1} \partial_X^2 R' + \frac{g_4}{g_1} \partial_X^4 R' + \frac{g_5}{g_2} \partial_X^2 R'^3\right]\end{aligned} \tag{31}$$

After ignoring the $O(\varepsilon)$, the mKdV equation with a kink solution can be obtained:

$$R_0'(X, T') = \sqrt{c} \tanh\left(\sqrt{\frac{c}{2}} (X - cT')\right) \tag{32}$$

Then, the $O(\varepsilon)$ correction is considered by assuming $R'(X, T') = R_0'(X, T') + \varepsilon R_1'(X, T')$. For the purpose of obtaining the propagation velocity c for the kink solution, the solvability condition should be satisfied. As $\left(R_0', M\left[R_0'\right]\right) \equiv \int_{-\infty}^{+\infty} dX' R_0' M\left[R_0'\right]$, where $M\left[R_0'\right] = \frac{g_3}{g_1} \partial_X^2 R' + \frac{g_4}{g_1} \partial_X^4 R' + \frac{g_5}{g_2} \partial_X^2 R'^3$. We get the general velocity c:

$$c = \frac{5 g_2 g_3}{2 g_2 g_4 - 3 g_1 g_5} \tag{33}$$

Subsequently, the general kink-antikink solution of the mKdV equation can be obtained:

$$\begin{aligned}\rho_j(t) = \rho_c &\pm \sqrt{\frac{g_1 c}{g_2} \left(\frac{\tau}{\tau_c} - 1\right)} \times \tanh \sqrt{\frac{c}{2} \left(\frac{\tau}{\tau_c} - 1\right)} \\ &\times \left[j + (1 - c g_1) \left(\frac{\tau}{\tau_c} - 1\right) t\right]\end{aligned} \tag{34}$$

5. Numerical simulation

In this section, numerical simulation is exhibited for the new lattice model, which investigates the influence of the traffic interruption probability on a gradient highway. Then the new lattice hydrodynamic model of Eq. (16) is discretized as follows:

$$\begin{aligned}&\rho_j(t + 2\Delta t) \\ &= 2\rho_j(t + \Delta t) - \rho_j(t) - a\Delta t \left[\rho_j(t + \Delta t) - \rho_j(t)\right] \\ &\quad - \Delta t^2 a \alpha_1 p \left[\rho_j(t) - \rho_j(t - \tau_0)\right] \\ &\quad - \Delta t^2 a \rho_0^2 A(\theta) \left[V_0\left(\rho_{j+1}, \theta\right) - V_0\left(\rho_j, \theta\right)\right] \\ &\quad + \Delta t^2 a \alpha_2 (1 - p)\end{aligned}$$

Table 2
The coefficients g_i of the model.

g_1	g_2	g_4
$\dfrac{\rho_c^2 A(\theta) V_0' + \alpha_1 p b^3 \tau_0^3 - 3\alpha_2 (1-p) b\tau_0 (1 - b\tau_0)}{6(1 + \alpha_1 p \tau_0)}$	$\dfrac{A(\theta) \rho_c^2 V_0'''}{6(1 + \alpha_1 p \tau_0)}$	$\dfrac{\rho_c^2 A(\theta) V_0'''}{12(1 + \alpha_1 p \tau_0)}$
g_5	g_3	
$\dfrac{\rho_c^2 A(\theta) V_0' + \alpha_1 p b^3 \tau_0^3 - 3\alpha_2 (1-p) b\tau_0 (1 - b\tau_0)}{6(1 + \alpha_1 p \tau_0)}$	$\dfrac{3\alpha_2 \tau_0 (1-p)}{\alpha_2 \tau_0 (1-p)(1 + \alpha_1 p \tau_0)^2 + (1 + \alpha_1 p \tau_0)^3 + (1 + \alpha_1 p \tau_0) \alpha_1 p \tau_0^2 \rho_c^2 A(\theta) V_0'}$	

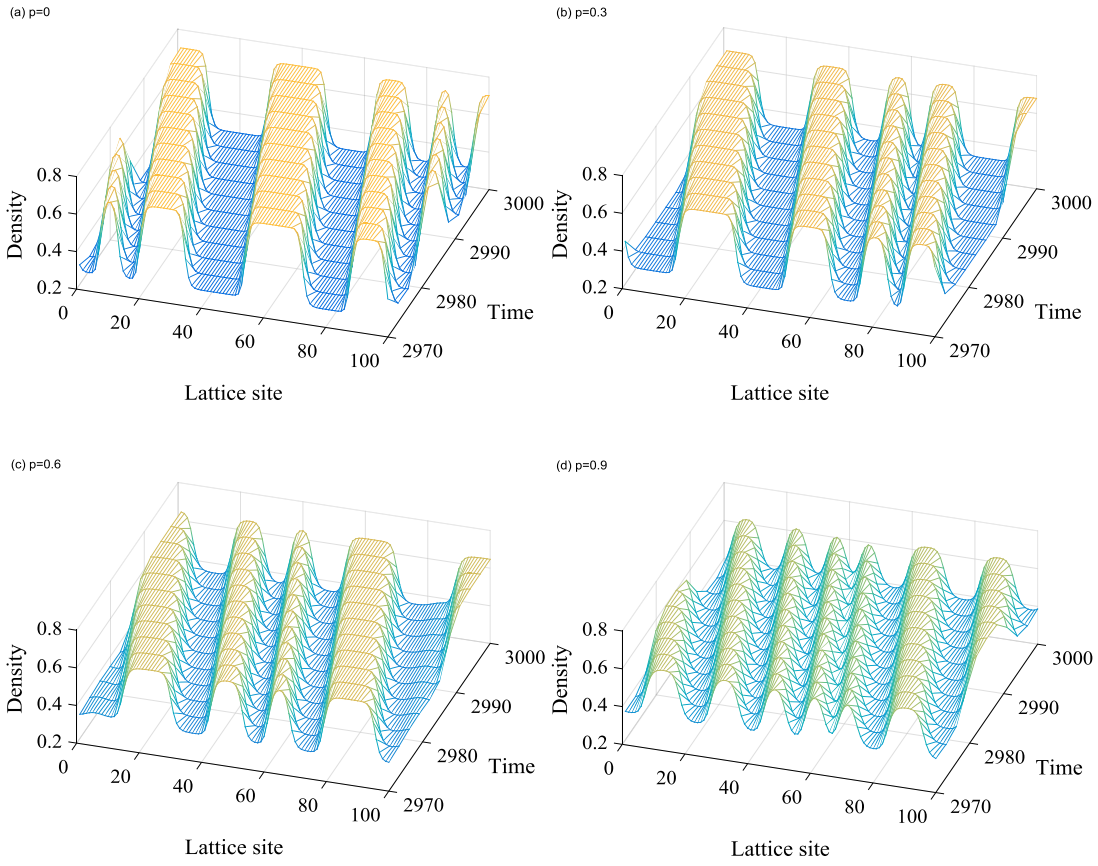

Fig. 3. The phase diagram of the model according to different values of parameter p.

$$\times \left[\rho_{j+1}(t) - \rho_{j+1}(t-\tau_0) - \rho_j(t) + \rho_j(t-\tau_0)\right] \tag{35}$$

where Δt is the difference time step of the equation.

Periodic boundary conditions can be given and the initial conditions are chosen as follows:

$$\rho_j(1) = \rho_j(0) = \begin{cases} \rho_0, & j \neq \dfrac{N}{2}, \dfrac{N}{2}+1, \\ \rho_0 - 0.05, & j = \dfrac{N}{2}, \\ \rho_0 + 0.05, & j = \dfrac{N}{2}, \end{cases} \tag{36}$$

where the total number of lattice $N = 100$, $t = 10^4$ s, $\alpha_1 = 0.5$, $\alpha_2 = 0.1$, $\rho_0 = \rho_c = 0.25$.

Fig. 3 shows the change trend of density with different values of traffic interruption probability when $\theta = 2°$. Fig. 3 (a)-(d) show the time evolution of density for $p = 0, 0.3, 0.6, 0.9$, respectively. From Fig. 3 (a) to (d), we can see that the amplitude of the density wave is continuously decreasing. And the phenomenon is very similar to the solution of the mKdV equation. Therefore, it is effective to consider the change of p on the stability of the lattice hydrodynamic model. In other words, considering the effect of the traffic interruption probability on a gradient highway can effectively alleviate traffic congestion.

Fig. 4 shows the density distribution when $t = 10300$ s, which corresponds to Fig. 3, when $\theta = 2°$, the amplitude of density wave decreases as the value of p increases. This shows that the traffic interruption probability can develop the stability of traffic flow greatly. Generally speaking, the effect of traffic interruption probability on a gradient highway should be considered in the lattice hydrodynamic model to enhance the stability of traffic flow.

Fig. 5 shows the traffic patterns with different values of θ in an uphill situation when $p = 0.6$. It is clear from Fig. 5 (a) that the amplitude of density wave is strong for $\theta = 0°$ in the stable region, and the traffic flow becomes skimble-scamble. When the value of θ increases from 0° to 6°, the amplitude of traffic waves decreases. Consequently, the non-uniform traffic flow evolves into a uniform and stable state when $\theta = 6°$. It also means that the traffic congestion can be decreased when considering the slope in an uphill situation.

In Fig. 6, the profile of the densities at time $t = 10300$ s is shown. The amplitudes of the densities decreased when increasing the value of θ. When the factor of gradient highway is efficient, the traffic congestions can be decreased in an uphill situation.

In Fig. 7, it shows the traffic patterns with different values of θ in a downhill situation when $p = 0.6$, the patterns (a), (b), (c) and (d) exhibit the kink-antikink density waves. When the value of θ increases from 0° to 6°, the amplitude of the density waves increases., and it reaches its maximum state as the slope grows to 6°. Therefore, the higher the gradient, the less stable the traffic flow in a downhill situation. And it is necessary to considerate the effect of gradient highway in real traffic.

In Fig. 8, a two-dimensional diagram of density at time $t = 10300$ s is shown. The amplitudes of the densities increase with the increasing the value of α. It can be also seen that the introduction of gradient highway into the traffic flow system can reduce traffic congestions.

In the above analysis, when the effect of traffic interruption probability and the gradient highway are respectively considered, the density curve of traffic flow has obvious fluctuation. That is to

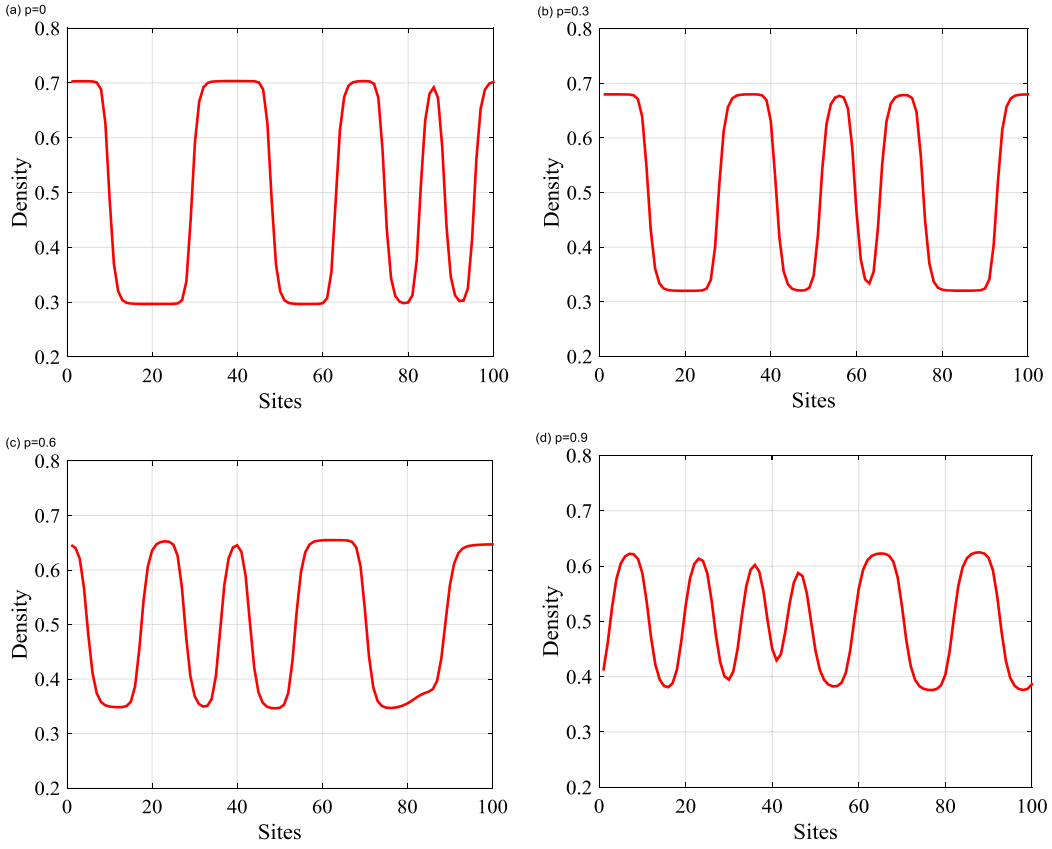

Fig. 4. The density profile at time $t = 10300\ s$ under the different values of p.

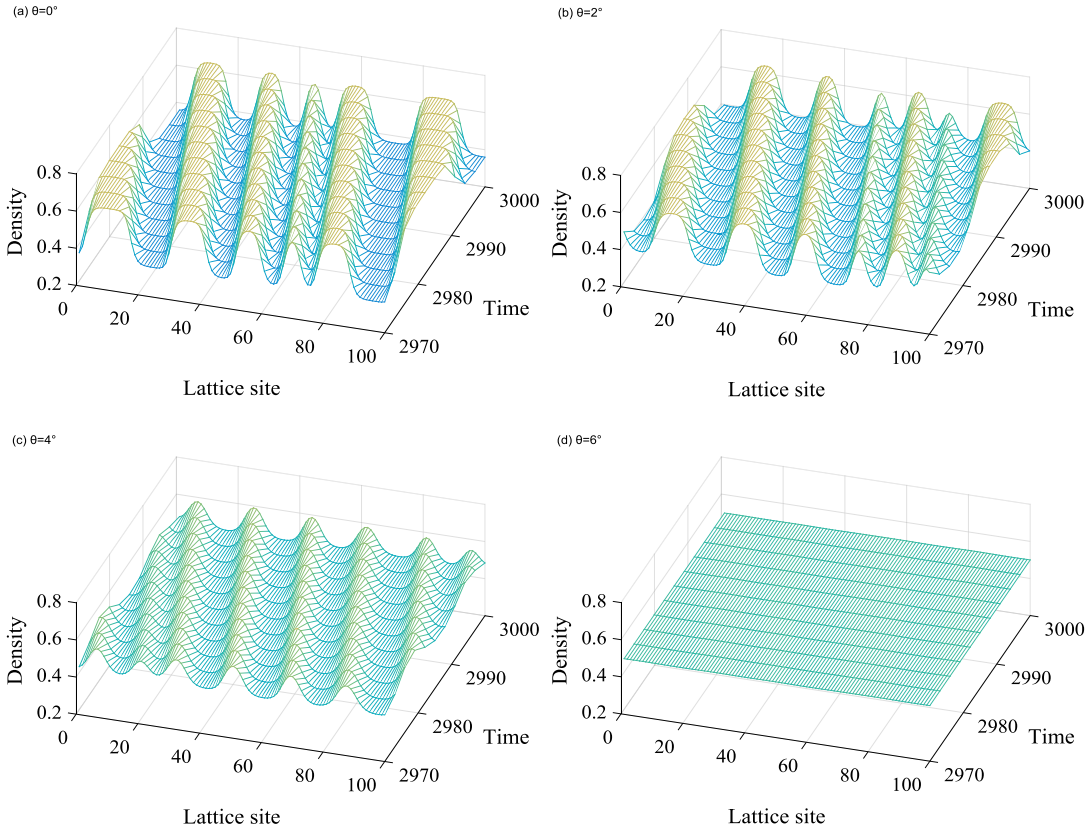

Fig. 5. The phase diagram o with different values of parameter θ for uphill situation.

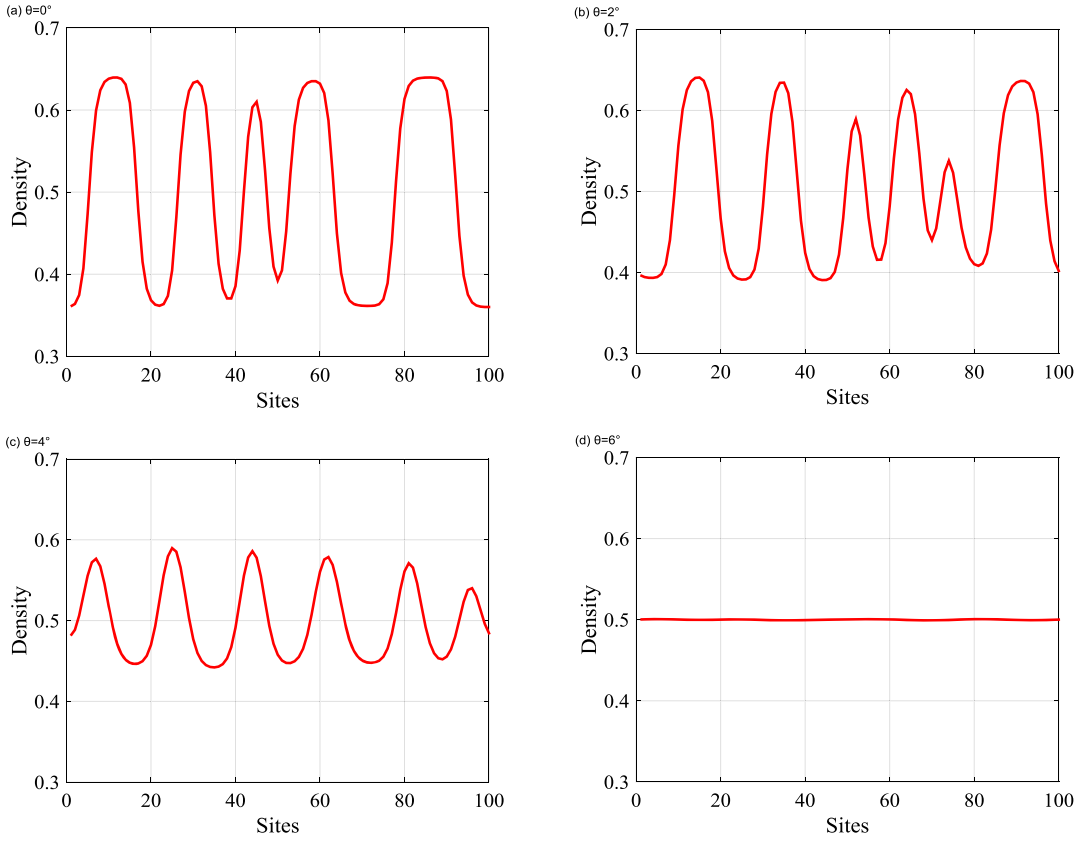

Fig. 6. The density profile at time $t = 10300\ s$ under the different values of θ for uphill situation.

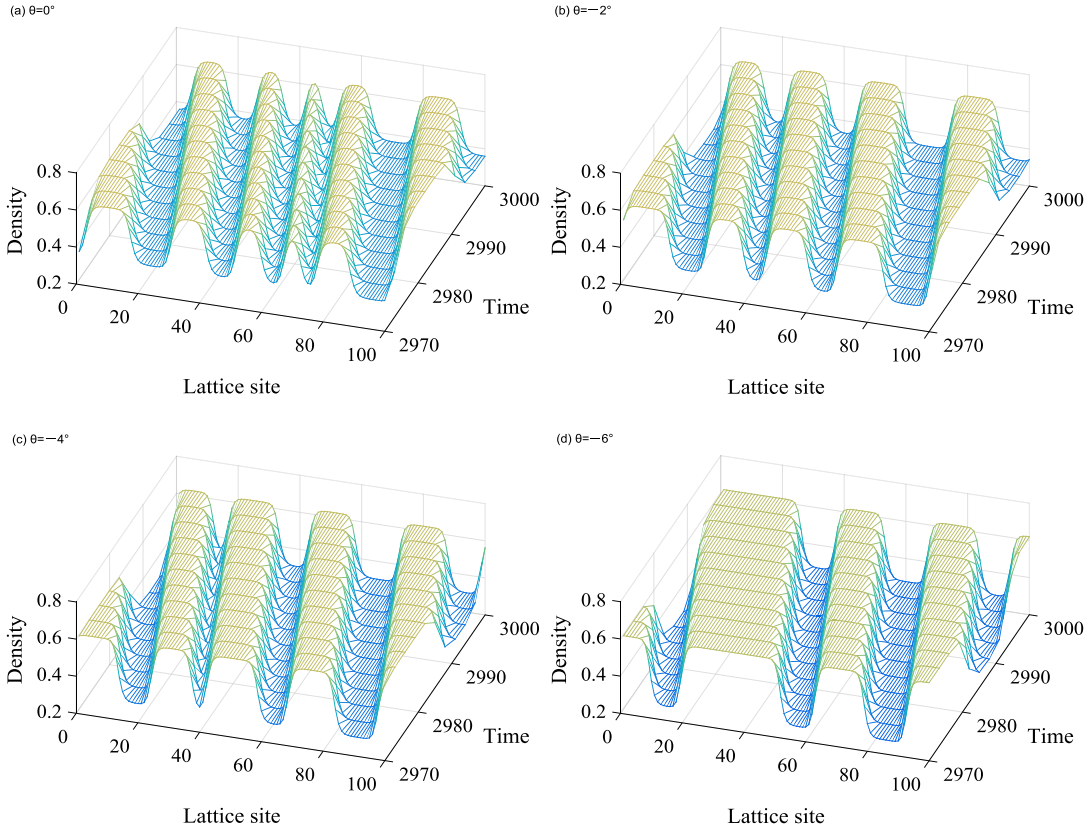

Fig. 7. The phase diagram with different values of parameter θ for downhill situation.

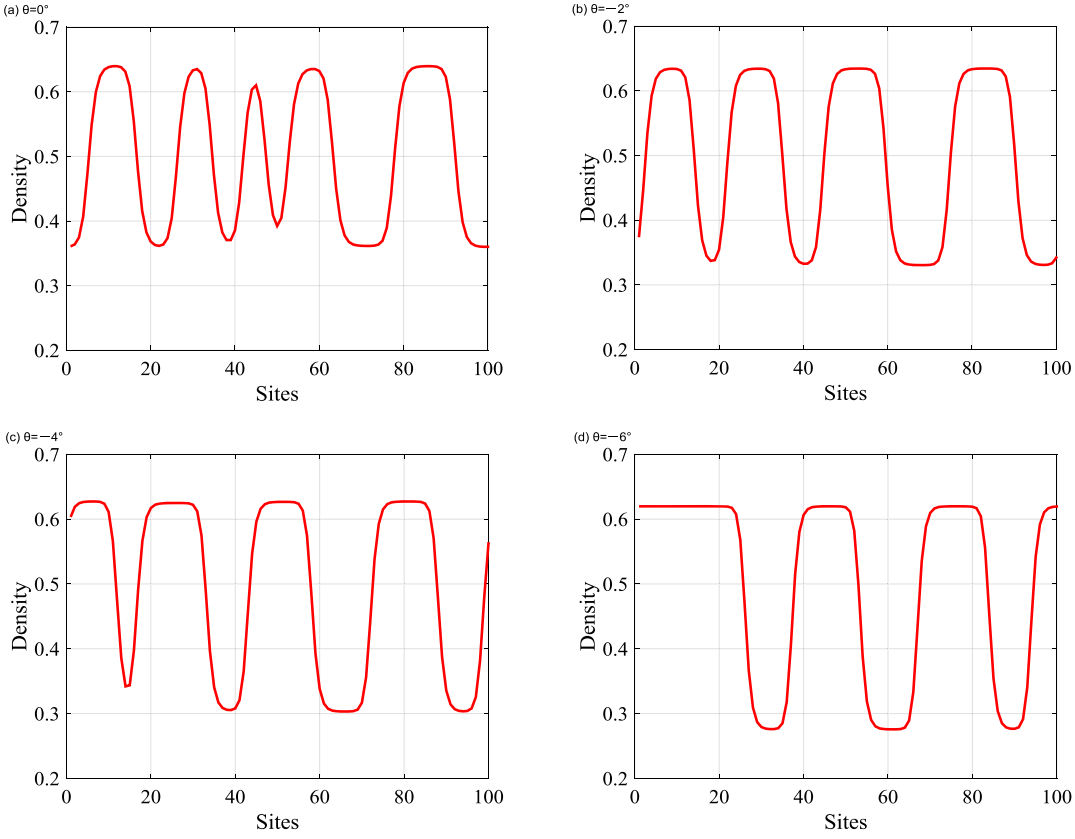

Fig. 8. The density profile at time $t = 10300\ s$ under the different values of θ for downhill situation.

say, in the study of traffic flow, the traffic interruption probability and the angle of slope can effectively alleviate traffic congestion.

6. Conclusion

We proposed an extended lattice hydrodynamic model by taking the traffic interruption probability into account on a gradient highway. The stability condition can be obtained by the use of linear analysis. The result of the stability analysis shows that the effect of traffic interruption probability on a gradient highway can enhance the stability of traffic flow. Through nonlinear stability analysis, we derived the kink-antikink solution of the mKdV equation to describe the traffic flow near the critical point. Phase diagram in the density-sensitivity space is given for different values of coefficients of the traffic interruption probability effect and the slope of the gradient highway. On the situation of different parameters in the novel model, a series of simulation are carried out. Numerical simulation shows that the effect of the traffic interruption probability plays an important role in enhancing the stability of the traffic flow on a gradient highway. And the numerical results are consistent with the results of linear and nonlinear analysis. It also shows that the traffic flow can be developed and the traffic jams can be suppressed by accounting for the traffic interruption probability on a gradient highway.

Acknowledgements

This work is supported by the National Natural Science Foundation of China (Grant No. 71571107) and the K.C. Wong Magna Fund in Ningbo University, China.

References

[1] M. Bando, K. Hasebe, A. Nakayama, A. Shibata, Y. Sugiyama, Dynamics model of traffic congestion and numerical simulation, Phys. Rev. E 51 (1995) 1035–1042.
[2] T.Q. Tang, W.F. Shi, H.Y. Shang, Y.P. Wang, A new car-following model with consideration of inter-vehicle communication, Nonlinear Dyn. 76 (2014) 2017–2023.
[3] H. Song, H.X. Ge, F.Z. Chen, R.J. Cheng, TDGL and mKdV equations for car-following model considering traffic jerk and velocity difference, Nonlinear Dyn. 87 (2017) 1809–1817.
[4] X. Wu, X.M. Zhao, H.S. Song, Q. Xin, S.W. Yu, Effects of the prevision relative velocity on traffic dynamics in the ACC strategy, Physica A 515 (2019) 192–198.
[5] W.X. Zhu, L.D. Zhang, Analysis of car-following model with cascade compensation strategy, Physica A 449 (2016) 265–274.
[6] W.X. Zhu, D.Z. Li, A new car-following model for autonomous vehicles flow with mean expected velocity field, Physica A 492 (2018) 2154–2165.
[7] W.X. Zhu, H.M. Zhang, Analysis of mixed traffic flow with human-driving and autonomous cars based on car-following model, Physica A 496 (2018) 274–285.
[8] W.X. Zhu, D. Jun, L.D. Zhang, A compound compensation method for car-following model, Commun. Nonlinear Sci. Numer. Simul. 39 (2016) 427–441.
[9] H. Ou, T.Q. Tang, An extended two-lane car-following model accounting for inter-vehicle communication, Physica A 495 (2018) 260–268.
[10] S.W. Yu, J.J. Tang, Q. Xin, Relative velocity difference model for the car-following theory, Nonlinear Dyn. 91 (2018) 1415–1428.
[11] Q. Xin, N.Y. Yang, R. Fu, S.W. Yu, Z.K. Shi, Impacts analysis of car following models considering variable vehicular gap policies, Physica A 501 (2018) 338–355.
[12] S.W. Yu, M.X. Huang, J. Ren, Z.K. Shi, An improved car-following model considering velocity fluctuation of the immediately ahead car, Physica A 449 (2016) 1–17.
[13] A. Kumar, Cellular automation: a discrete approach for modeling and simulation of artificial life systems, Int. J. Sci. Res. Publ. 3 (2013) 2250–3153.
[14] T.Q. Tang, Y.X. Rui, J. Zhang, H.Y. Shang, A cellular automation model accounting for bicycle's group behavior, Physica A 492 (2018) 1782–1797.
[15] H. Qu, T.Q. Tang, J. Zhang, J.M. Zhou, A macro traffic flow model with probability distribution function, Phys. Lett. A 382 (2018) 2819–2824.
[16] R.J. Cheng, H.X. Ge, F.X. Sun, J.F. Wang, An extended macro model accounting for acceleration changes with memory and numerical tests, Physica A 506 (2018) 270–283.

[17] G.H. Peng, S.H. Yang, H.Z. Zhao, The difference of drivers' anticipation behaviors in a new macro model of traffic flow and numerical simulation, Phys. Lett. A 382 (2018) 2595–2597.
[18] T.Q. Tang, H.J. Huang, H.Y. Shang, An extended macro traffic flow model accounting for the driver's bounded rationality and numerical tests, Physica A 468 (2017) 322–333.
[19] R.J. Cheng, H.X. Ge, J.F. Wang, KdV-Burgers equation in a new continuum model based on full velocity difference model considering anticipation effect, Physica A 481 (2017) 52–59.
[20] R.J. Cheng, H.X. Ge, J.F. Wang, An extended continuum model accounting for the driver's timid and aggressive attributions, Phys. Lett. A 381 (2017) 1302–1312.
[21] R.J. Cheng, H.X. Ge, J.F. Wang, An extended macro traffic flow model accounting for multiple optimal velocity functions with different probabilities, Phys. Lett. A 381 (2017) 2608–2620.
[22] Q.T. Zhai, H.X. Ge, R.J. Cheng, An extended continuum model considering optimal velocity change with memory and numerical tests, Physica A 490 (2018) 774–785.
[23] R.J. Cheng, H.X. Ge, J.F. Wang, The nonlinear analysis for a new continuum model considering anticipation and traffic jerk effect, Appl. Math. Comput. 332 (2018) 493–505.
[24] R.J. Cheng, Y.N. Wang, An extended lattice hydrodynamic model considering the delayed feedback control on a curved road, Physica A 513 (2019) 510–517.
[25] C.T. Jiang, H.X. Ge, R.J. Cheng, Mean-field flow difference model with consideration of on-ramp and off-ramp, Physica A 513 (2019) 465–467.
[26] G.H. Peng, H. Kuang, L. Qing, Feedback control method in lattice hydrodynamic model under honk environment, Physica A 509 (2018) 651–656.
[27] S.D. Qin, Z.T. He, R.J. Cheng, An extended lattice hydrodynamic model based on control theory considering the memory effect of flux difference, Physica A 509 (2018) 809–816.
[28] G.H. Peng, S.H. Yang, H.Z. Zhao, A delayed-feedback control method for the lattice hydrodynamic model caused by the historic density difference effect, Physica A 509 (2018) 855–860.
[29] H.X. Ge, R.J. Cheng, The "backward looking" effect in the lattice hydrodynamic model, Physica A 387 (2008) 6952–6958.
[30] H.X. Ge, P.J. Zheng, S.M. Lo, R.J. Cheng, TDGL equation in lattice hydrodynamic model considering driver's physical delay, Nonlinear Dyn. 76 (2014) 441–445.
[31] T. Nagatani, Modified KDV equation for jamming transition in the continuum models of traffic, Physica A 271 (1998) 599–607.
[32] T.Q. Tang, J. Zhang, K. Liu, A speed guidance model accounting for the driver's bounded rationality at a signalized intersection, Physica A 473 (2017) 45–52.
[33] C.T. Jiang, R.J. Cheng, H.X. Ge, Effects of speed deviation and density difference in traffic lattice hydrodynamic model with interruption, Physica A 506 (2018) 900–908.
[34] Z.Z. Liu, J.F. Wang, H.X. Ge, KdV-Burgers equation in the modified continuum model considering the "backward looking" effect, Nonlinear Dyn. 91 (2018) 2007–2017.
[35] Z.H. Wang, R.J. Cheng, R.J. Cheng, Nonlinear analysis for a modified continuum model considering driver's memory and backward looking effect, Physica A 508 (2018) 18–27.
[36] D.L. Fan, Y.C. Zhang, Y. Shi, Y. Xue, F.P. Wei, An extended continuum traffic model with the consideration of the optimal velocity difference, Physica A 508 (2018) 402–413.
[37] Z.Z. Jin, Z.P. Li, R.J. Cheng, H.X. Ge, Nonlinear analysis for an improved car-following model account for the optimal velocity changes with memory, Physica A 507 (2018) 278–288.
[38] G.H. Peng, X.H. Cai, C.Q. Liu, B.F. Cao, M.X. Tuo, Optimal velocity difference model for a car-following theory, Phys. Lett. A 375 (2011) 3973–3977.
[39] J. Zhou, Z.K. Shi, J.L. Cao, Nonlinear analysis of the optimal velocity difference model with reaction-time delay, Physica A 396 (2014) 77–87.
[40] T.Q. Tang, C.Y. Li, H.J. Huang, H.Y. Shang, An extended optimal velocity model with consideration of honk effect, Commun. Theor. Phys. 54 (2010) 1151–1155.
[41] G.H. Peng, S.H. Yang, D.X. Xia, X.Q. Li, A novel lattice hydrodynamic model considering the optimal estimation of flux difference effect on two-lane highway, Physica A 506 (2018) 929–937.
[42] G.H. Peng, S.H. Yang, H.Z. Zhao, The difference of drivers' anticipation behaviors in a new macro model of traffic flow and numerical simulation, Phys. Lett. A 382 (2018) 2595–2597.
[43] G.H. Peng, S.H. Yang, D.X. Xia, X.Q. Li, Impact of lattice's self-anticipative density on traffic stability of lattice model on two lanes, Nonlinear Dyn. 94 (2018) 1–9.
[44] G. Zhang, D.H. Sun, H. Liu, D. Chen, Stability analysis of a new lattice hydrodynamic model by considering lattice's self-anticipative density effect, Physica A 486 (2017) 806–813.
[45] Y.K. Wei, H. Yang, H.S. Dou, Z. Lin, Z.D. Wang, A novel two-dimensional coupled lattice Boltzmann model for thermal incompressible flow, Appl. Math. Comput. 339 (2018) 556–567.
[46] T.Q. Tang, X.F. Luo, J. Zhang, L. Chen, Modeling electric bicycle's lane-changing and retrograde behaviors, Physica A 490 (2018) 1377–1386.
[47] C.X. Ma, W. Hao, R.C. He, X.Y. Jia, F.Q. Pan, J. Fan, R.Q. Xiong, Distribution path robust optimization of electric vehicle with multiple distribution centers, PLoS ONE 13 (3) (2018) e0193789.
[48] C.X. Ma, W. Hao, F.Q. Pan, W. Xiang, Road screening and distribution route multi-objective robust optimization for hazardous materials based on neural network and genetic algorithm, PLoS ONE 13 (6) (2018) e0198931.
[49] C.X. Ma, R.C. He, W. Zhang, Path optimization of taxi carpooling, PLoS ONE 13 (8) (2018) e0203221.
[50] J. Zhou, Z.K. Shi, Lattice hydrodynamic model for traffic flow on curved road, Nonlinear Dyn. 83 (2016) 1217–1236.
[51] Y.D. Jin, J. Zhou, Z.K. Shi, Lattice hydrodynamic model for traffic flow on curved road with passing, Nonlinear Dyn. 89 (2017) 107–124.
[52] R. Kaur, S. Sharma, Analysis of driver's characteristics on a curved road in a lattice model, Physica A 471 (2017) 59–67.
[53] P. Redhu, A.K. Gupta, Phase transition in a two-dimensional triangular flow with consideration of optimal current difference effect, Nonlinear Dyn. 78 (2014) 957–968.
[54] T. Nagatani, Jamming transition in traffic flow on triangular lattice, Physica A 271 (1999) 200–221.
[55] A.K. Gupta, S. Sharma, P. Redhu, Analyses of lattice traffic flow model on a gradient highway, Commun. Theor. Phys. 62 (2014) 393.
[56] K. Komada, S. Masukura, T. Nagatani, Effect of gravitational force upon traffic flow with gradients, Physica A 388 (2009) 2880–2894.
[57] D.H. Sun, P. Tan, D. Chen, S. Cheng, L.H. Guan, Burgers and mKdV equation for car-following model with considering drivers' characteristics on a gradient highway, Int. J. Mod. Phys. B 32 (2018) 1850314.
[58] W.X. Zhu, R.L. Yu, Nonlinear analysis of traffic flow on a gradient highway, Physica A 391 (2012) 954–965.
[59] G.H. Peng, X.H. Cai, B.F. Cao, C.Q. Liu, A new lattice model of traffic flow with the consideration of the traffic interruption probability, Physica A 391 (2012) 656–663.